NJC

New Journal of Chemistry

A journal for new directions in chemistry

Accepted Manuscript

This article can be cited before page numbers have been issued, to do this please use: F. Isaia, A. Garau, M. C. Aragoni, M. Arca, C. Caltagirone, C. Castellano, F. Demartin, V. Lippolis and T. Pivetta, *New J. Chem.*, 2021, DOI: 10.1039/D0NJ05601D.

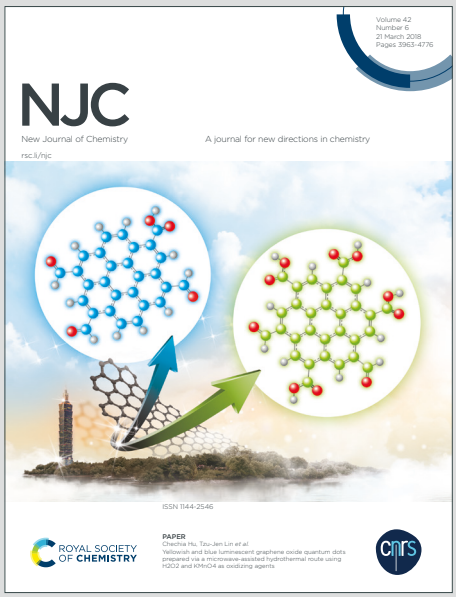

This is an Accepted Manuscript, which has been through the Royal Society of Chemistry peer review process and has been accepted for publication.

Accepted Manuscripts are published online shortly after acceptance, before technical editing, formatting and proof reading. Using this free service, authors can make their results available to the community, in citable form, before we publish the edited article. We will replace this Accepted Manuscript with the edited and formatted Advance Article as soon as it is available.

You can find more information about Accepted Manuscripts in the Information for Authors.

Please note that technical editing may introduce minor changes to the text and/or graphics, which may alter content. The journal's standard Terms & Conditions and the Ethical guidelines still apply. In no event shall the Royal Society of Chemistry be held responsible for any errors or omissions in this Accepted Manuscript or any consequences arising from the use of any information it contains.

Stabilization of caesium ions by simple organic molecules: crystal structures of Cs(OXL) (OXL = oxalurate anion), and CsOH/cyanuric acid co-crystal $Cs_3(CYH_3)_4(OH)_3$ (CYH_3 = cyanuric acid)

Francesco Isaia,*[a] Alessandra Garau,[a] Carlo Castellano,[b] Francesco Demartin,[b] M. Carla Aragoni,[a] Massimiliano Arca,[a] Claudia Caltagirone,[a] Vito Lippolis,[a] Tiziana Pivetta[a]

[a]Dipartimento di Scienze Chimiche e Geologiche, Università degli Studi di Cagliari, Cittadella Universitaria, Monserrato CA, 09042, Italy

[b]Dipartimento di Chimica, Università degli Studi di Milano, via Golgi 19, Milano, 20133, Italy.

The reaction in water between CsOH and parabanic acid (PBH_2) leads to the formation of the caesium salt of the oxalurate anion Cs(OXL), while the reaction with cyanuric acid (CYH_3) leads to the formation of CsOH co-crystal of cyanuric acid $Cs_3(CYH_3)_4(OH)_3$. The X-ray crystal structure of these compounds shows that both the organic moieties OXL and CYH_3 form robust homomeric ribbons based on strong and articulated N-H···O hydrogen bonds. The stabilization of the Cs^+ ions can occur regardless of whether the ribbon of organic units is negatively charged or neutral. In Cs(OXL), each cation displays nine-fold coordination with Cs-O distances in the range 2.975(3) - 3.601(4) Å; in $Cs_3(CYH_3)_4(OH)_3$, two of the Cs^+ cations (Cs1 and Cs2) display a nine-fold coordination with Cs-O distances in the range 3.007(9) – 3.823(13) Å and one (Cs3) is ten-fold coordinated with Cs-O distances in the range 3.161(14) – 3.653(17) Å. The molecular electrostatic potential maps of OXL and di-OXL anions have been reported and discussed.

Introduction

Stable caesium ion occurs naturally on Earth's crust at low concentration, mainly deriving from erosion of rocks and minerals; it is toxic to plants and causes a decrease in the growth of biomass and potassium starvation *via* competitive interaction with K^+ binding sites in proteins.[1a] An even more serious problem arises from the presence of caesium radioisotopes [^{134}Cs ($T_{1/2}$ = 2.06 yr) and ^{137}Cs ($T_{1/2}$ = 30.17 yr)] in the soil and on plant leaves as a result of atmospheric deposition following nuclear weapons testing, discharge of nuclear waste, and as well as accidental release from nuclear plants in the terrestrial environment.[1b-1e] When caesium metal comes into contact with water, a vigorous reaction occurs with the formation of caesium hydroxide. The mobility and bioavailability of Cs^+ ions in the environment is strongly influenced by its interaction/complexation with some constituents in soil humic substances (fulvic acids, humic acids and humins).[2] Fulvic and humic acids are complex

View Article Online
DOI: 10.1039/D0NJ05601D

organic systems[3] which can interact with metal ions, oxides, hydroxides, mineral and organic compounds to form both water-soluble and water-insoluble complexes. Through the formation of these complexes, metals and organics in soil and waters can be dissolved, mobilized, transported, or accumulated. [4-6] It goes without saying that any possible transfer of caesium radioisotopes to the terrestrial food chain poses a serious radiological hazard for human health.[1e]

The need for a better comprehension of the interaction between Cs^+ ions and organic functional groups present in soil organic matter (in particular –COOH/–COO^-, –OH/–O^-, –NH/N^-, and –NH_2), prompted us to study the interaction between CsOH and the amide-containing molecules parabanic acid (PBH_2) and cyanuric acid (CYH_3) (Fig. 1) to understand both their coordination tendencies, and the role of hydrogen bonding in the stabilization of the Cs-organic compounds. The acid-base reaction CsOH-PBH_2/CYH_3 instead of the expected formation of the deprotonated species of the acids considered, resulted in the formation of compounds Cs(OXL) [OXL = oxalurate anion] and $Cs_3(CYH_3)_4(OH)_3$, the crystal structure of which is reported.

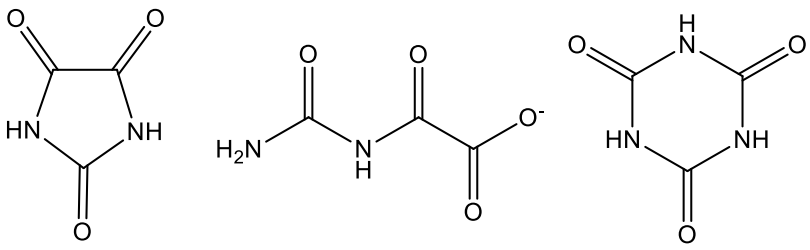

PBH_2 OXL CYH_3

Fig. 1 Parabanic acid (PBH_2), oxalurate anion (OXL) and (iso)cyanuric acid (CYH_3) structural formulas.

Results and Discussion

Reactivity of parabanic acid with CsOH.

The reaction between parabanic acid and CsOH was carried out in water by adding drop-by-drop a caesium hydroxide solution to a suspension of parabanic acid, imposing a final reaction pH not exceeding 10. After one hour stirring, the solution was filtered, and slowly concentrated in a desiccator to produce a white microcrystalline solid compound, identified by its elemental analysis and single crystal X-ray diffraction to be the caesium salt of the oxalurate anion Cs(OXL), Fig. 1. The oxalurate anion formation is in accordance with the general reaction reported in Scheme 1 (see also ESI – Scheme S1). It is of interest to note that no water or isopropyl alcohol as ligands

View Article Online
DOI: 10.1039/D0NJ05601D

originating from the solvents used in the salt preparation/crystallization were present in the separated crystals.

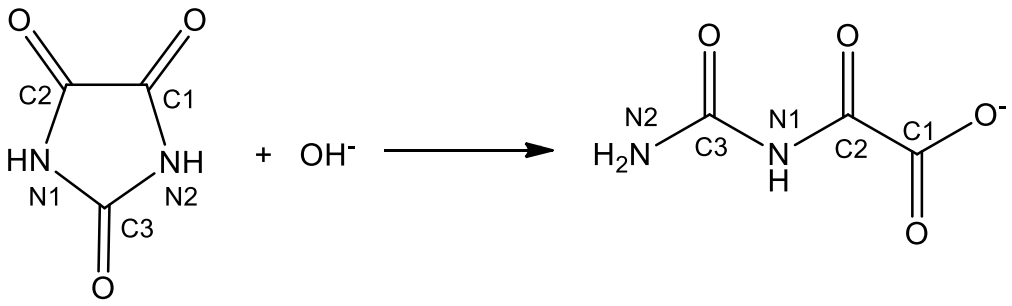

Scheme 1. Oxalurate anion formation from the reaction between parabanic acid and the hydroxide ion. T = 20 °C, pH = 10; reaction time: 1 hour.

The oxalurate anion possesses structural and topological properties that make it a versatile ligand to form supramolecular structures. The rotation around the bonds that form the backbone of the molecule (N2-C3-N1-C2-C1) can produce different conformations including the planar one.[7] The oxalurate features four oxygen atoms and two amine nitrogen atoms which can behave as hydrogen-bond acceptors and hydrogen-bond donors, respectively. Moreover, one or more of these six donor atoms can bind to metal centres in three distinct coordination modes, namely, chelating, terminal, or bridging coordination.[8]

Crystal Structure of Cs(OXL) (1)

The positive charged nature of *caesium* metal ion along with its large cationic radius leads to the formation of coordination networks characterized by strong interactions with molecules containing oxygen atoms. Generally, caesium ion displays high coordination numbers that generally dominate its structural coordination chemistry. Moreover, the large electronegativity difference between the caesium metal center and carboxylate oxygen atoms imposes strong ionic character to the Cs-O bond. Given that caesium ions are generally considered as hard cations, they interact preferably with oxygen donor atoms rather than nitrogen atoms. However, when oxygen donors are not available in sufficient quantity to satisfy the coordination of the metal ions, nitrogen atoms can also be involved in metal ion coordination.[9]

The Cs−O bonds, as reported in the ICDS data bank,[10] feature a wide range of lengths ranging from 2.46 Å to 3.60 Å. The preferential coordination numbers adopted by the caesium ions are 8, 9, and 10; however other values from 1 to 12 also exist.[11]

The asymmetric unit of compound (**1**) contains two independent Cs^+ cations and two oxalurate anions.

View Article Online
DOI: 10.1039/D0NJ05601D

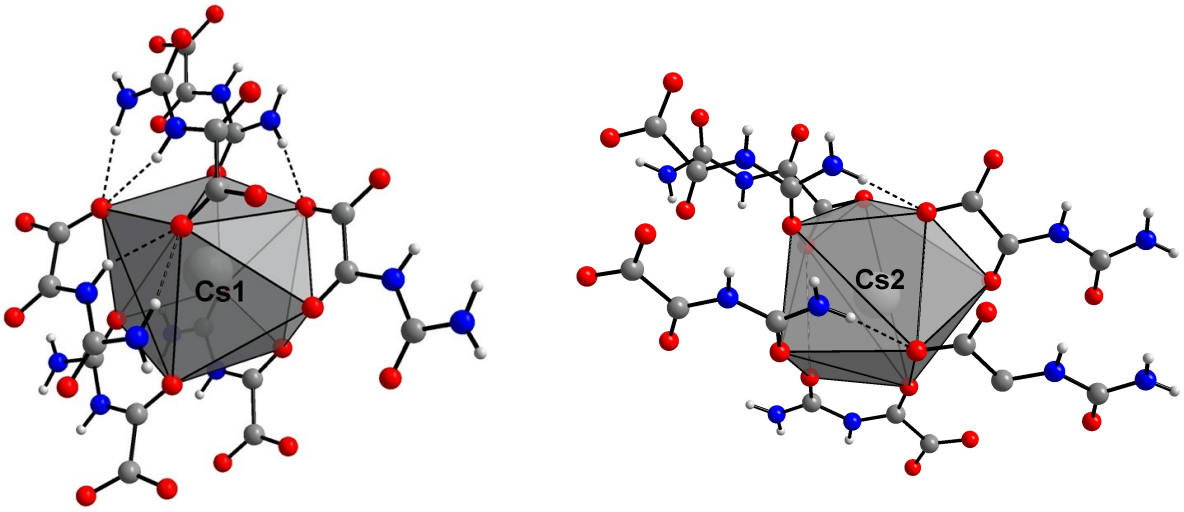

Fig. 2 The coordination environment of the two independent Cs cations in Cs(OXL) (**1**)

Each cation displays nine-fold coordination with Cs-O distances in the range 2.975(3) - 3.601(4) Å (Fig. 2, ESI-Table S2), which are well within the range reported in the literature for other caesium complexes.[11] Caesium cations are arranged to form layers almost stacked along [100], surrounded on both sides by planar oxalurate anions that complete the coordination sphere of the cations and are aligned along [010] to form ribbons held together by hydrogen bonds, (Fig. 3, ESI-Figure S1 and -Figure S2; ESI-Table S2). In the crystal structure, each oxalurate anion is linked to three others of the same species by hydrogen bonds to form a double flat ribbon.

The strong interactions between the two chains are based on the presence of four hydrogen bonds formed between two neighbouring oxalurates (Fig. 4) arising from the mutual interaction between oxygens atom O2/O6 as acceptors and the amide (N1/N3) and amino groups (N2/N4). Two additional intermolecular hydrogen bonds [the N1-H···O2 and N3-H···O6] contribute to maintain the almost planarity of the oxalurate anions; Table 1 collects the intramolecular and intermolecular hydrogen bond distances and angles. The propagation of the ribbon is based on the formation of hydrogen bonds [HN-H···O(C)] between adjacent anions.

View Article Online
DOI: 10.1039/D0NJ05601D

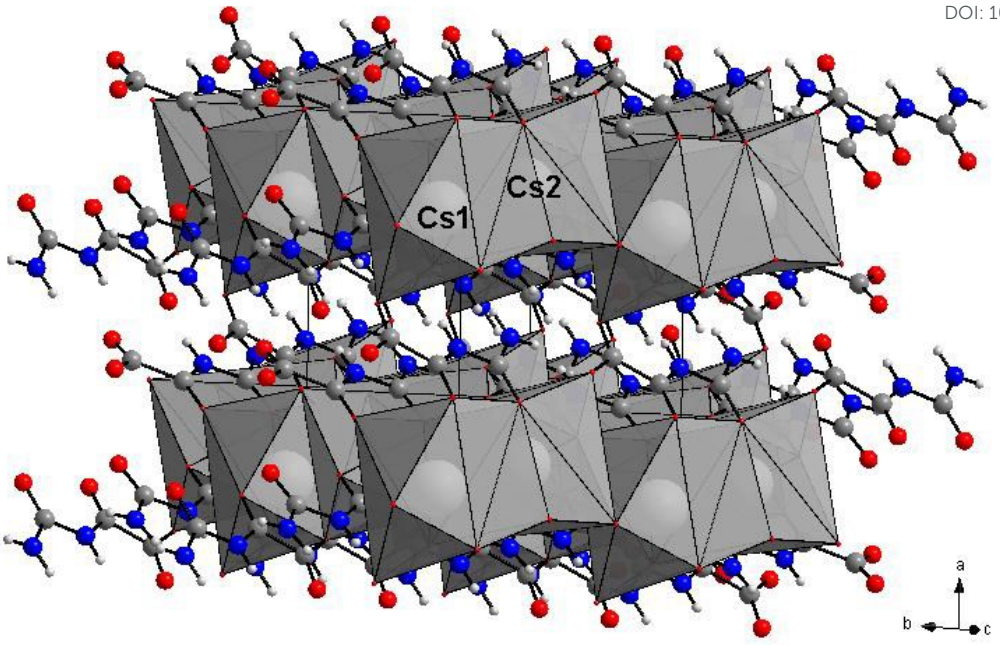

Fig. 3 Perspective view of Cs(OXL) (**1**) with the Cs coordination polyhedra highlighted.

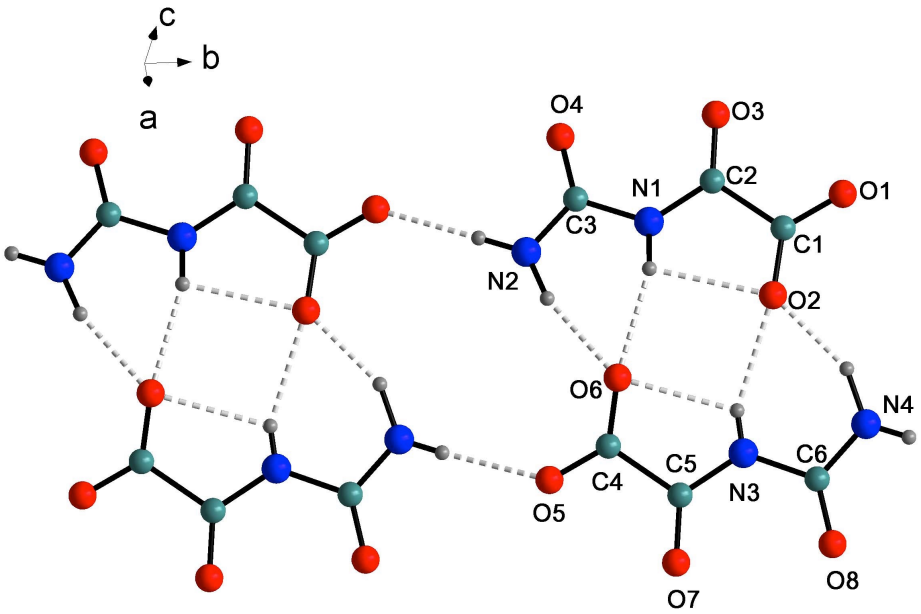

Fig. 4 Drawing of the double ribbon formed by self-assembly of oxalurate anions. Interatomic distances (Å) are O1-C1 1.241(5), O2-C1 1.255(5), O3-C2 1.219(5), O4-C3 1.226(5), N1-C2 1.356(6), N1-C3 1.403(6), N2-C3 1.328(6), C1-C2 1.556(6), O5-C4 1.234(6), O6-C4 1.258(5), O7-C5 1.218(5), O8-C6 1.223(5), N3-C5 1.369(6), N3-C6 1.420(6), N4-C6 1.327(6), C4-C5 1.567(6). Hydrogen bonding interactions are depicted as dashed lines.

Table 1. Hydrogen bonds (Å and deg.) in Cs(OXL) (**1**)

N1···O2	2.648(5)	N1-H1···O2	101.1(3)
N3···O6	2.650(5)	N3-H3···O6	108.2(3)
N2···O6f	2.902(5)	N2-H2B··O6f	156.1(3)
N1···O6f	2.972(5)	N1-H1···O6f	155.6(3)
N3···O2f	2.895(6)	N3-H3···O2f	153.4(3)
N4···O2f	2.875(5)	N4-H4B···O2f	153.0(3)
N4-O5g	2.849(6)	N4-H4A···O5g	171.7(3)
N2-O1g	2.878(6)	N2-H2A···O1g	170.9(3)

Symmetry codes: a = 1- x,1-y,1-z; b = -x, 1-y,1-z; c = x, 1+y, z; d = x, y, z+1; e = -x, 2-y, -z; f = 1-x, 1-y, -z; g = x, y-1, z.

Quantum mechanical calculations

DFT quantum mechanical calculations were carried out to determine the energy relative to the most stable forms of the OXL anion. B3LYP as the density functional theory functional and 6-31G** as the basis set were selected to predict geometry and some chemical features. They highlighted two geometries both characterized by the presence of an intramolecular interaction: a bent geometry featuring the O1/O2···H-N2 interaction and a planar geometry featuring the O1/O2···H-N1 interaction, (ESI-Table S2). The difference in energy between the two forms clearly indicates that the planar one was more stable both in the gas phase and in water solution ($E_{\mathrm{OXLplanar}}$ - E_{OXLbent} = -71.6 kJ/mol). The greater stability of the OXL anion planar form makes easier the formation of four hydrogen bonds between two OXL anions. The calculated energy gain of the di-OXL anion formation process from two planar OXL anions is low (2 x $E_{\mathrm{OXL\ planar}}$ - $E_{\mathrm{di\text{-}OXL}}$ = -52.5 kJ/mol), conversely the solvation energy is markedly increased (2x$E_{\mathrm{OXL\ planar}}$ - $E_{\mathrm{di\text{-}OXL}}$ = 310.83 kJ / mol).

Molecular electrostatic potential (MEP) maps

The molecular electrostatic potential (MEP) map is a useful descriptor for determining molecules' reactive behavior, especially in noncovalent interactions.[12,13] The electrostatic potential $V(\mathbf{r})$ is a physical observable that can be determined computationally.[13] The values of the electrostatic potential (kJ/mol) at the surface are represented by different colors: electrostatic potential increases in the order red < orange < yellow < green < blue, and specify the electron rich, slightly electron rich, slightly electron deficient, and electron deficient regions, respectively. Figure 5A shows that OXL has several regions of negative surface potential $V_s(r)$. They are associated with the lone-pairs of the imino and amino nitrogens and the carbonyl/carboxyl oxygens. An extended electron rich region (red)

overlaps the four oxygen atoms O2, O1, O3, and O4 with each other. The shield of electrostatic potential that range from approx. -661 kJ/mol to approx. -35 kJ/mol enables interactions with metal cationic species, indicating these oxygens as potential hydrogen bond acceptors. The electron deficient (blue) region on N1H and $N2H_2$ hydrogens is due to their binding to the nitrogen. These hydrogens are suitable N-H hydrogen bonding sites, the formation of the intramolecular hydrogen bond (N1-H···O2) is associated with a yellow-green colouring between the nitrogen-oxygen atoms.

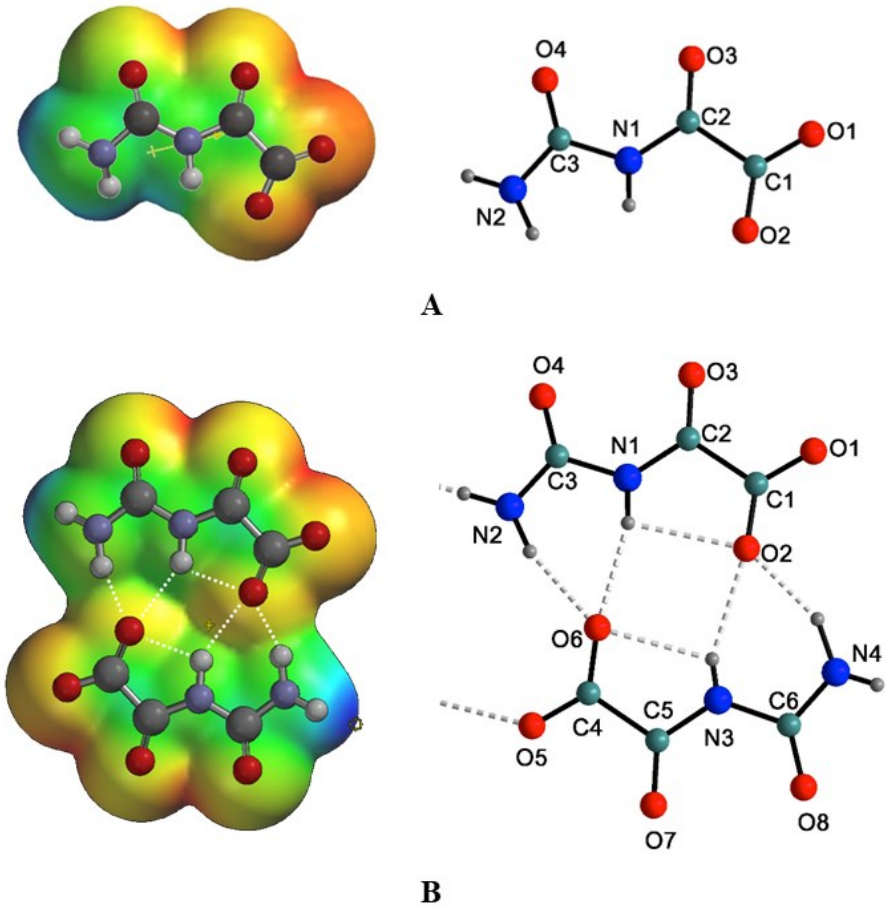

Fig. 5 Electrostatic potential surface maps (left), and atoms numbering (right) of OXL anion (**A**) and di-OXL anion (**B**). Red areas refer to regions containing electron-rich and blue areas refer to the regions containing electron-poor sites (from -660.828 kJ/mol to -35.766 kJ/mol for **A**, from -838.616 kJ/mol to -302.460 kJ/mol for **B**).

The calculated electrostatic potentials map of di-OXL anion is shown in Fig. 5B. The di-anion is the result of four O···H intermolecular interactions with the O···N interactions in the range 2.875 to 2.972 Å and two intramolecular hydrogen bonding N1-H···O3 and N3-H···O6 that ensure the planarity of the di-anion. The di-OXL anion formation leads to an interaction energy ($E_{\text{di-OXL}}$ –2 x E_{OXL}) at 0 K of +14933 kJ/mol in gas phase and of +14802 kJ/mol in water phase, while at 298.15 K the two values are +14931 kJ/mol and +14797 kJ/mol, respectively. The space involved in the

formation of the six hydrogen bonds takes on a yellow-green colouring since the difference in potential between nitrogen/oxygen atoms and hydrogen atoms, which is the driving force for the formation of the intermolecular/intramolecular bonds, will be partially lowered by the hydrogen bonding interactions.[12-14] Finally, the map correctly shows two blue zones which are related to one of the two hydrogens present in the amino groups N2 and N4, and which are involved in the formation of chains N-H···O with adjacent molecules. So, the electrostatic potential maps confirm their usefulness in showing the suitable sites for the formation of hydrogen bonding. Sites that correspond to those reported in the structure of the Cs(OXL) salt.

The atomic charges calculated with ab initio methods are reported in ESI-Table S4 and ESI-Table S5 for the planar and bent forms of OXL, and in ESI-Table S6 those for the di-OXL anion. The Natural Population Analysis charges localized on the different atoms vary for the planar form of OXL in the order N2> O2> N1> O1> O4> O3 (negative charges) and C3> C1> C2 (positive charges) and for di-OXL in the order (N2, N4) > (O2, O6) > (N1, N3) > (O1, O5) > (O4, O8) > (O3, O7) (negative charges), (C3, C6) > (C1, C4) > (C2, C5) > (positive charges).

In di-OXL anion, the distribution of the charges shows the effects on the atoms of the hydrogen bonds that unite the two anions. All the oxygens show an increase of the negative charge with the higher value shown by O2/O6 engaged in the formation of three hydrogen bonds. The effects resulting from the formation of di-OXL are both to stabilize the conformation of this species and, from the point of view of electronic charges, to increase the capacity of the oxygen to interact electrostatically with electropositive species.

Reactivity of (iso)cyanuric acid with CsOH

(Iso)cyanuric acid[15] (CYH_3) is a polyfunctional small molecule that has a commercial and industrial importance, it is commonly used as chlorine stabilizer in the swimming pools, Fig. 1.[16] Cyanuric acid is a symmetrical molecule (D_{3h} symmetry) that can exist in the keto and enol tautomers with the former predominantly observed in the solid state.[17,18] It features the presence of three hydrogen bonding acceptor $O_{C=O}$ sites and three hydrogen bonding donor N-H sites that make it capable of participating in multiple hydrogen bonds by interacting with molecules possessing a "complementary" structure in terms of hydrogen bonding capacity.[19,20]

As reported by Nichol *et al*., the coordination chemistry of CYH_3 towards metal ions carried out in aqueous solutions is markedly dependent on the relative amount and type of base used.[16,21] In fact, mono-deprotonation (pKa = 6.85) is easily achievable forming the CYH_2^- anion, whereas double deprotonation requires a control of the reaction conditions (pKa = 10.91) forming CYH^{2-},

and triple deprotonation (pKa > 12) is uncommon as it requires a suitable metal complex to stabilize the CY^{3-} anion. Only a few crystalline structures of metal ions with cyanurate ions (CYH_2^-/CYH^{2-}/CY^{3-}) are reported in the literature,[16,21,] and even fewer in the case of cyanuric acid.[22]

The reaction between cyanuric acid and caesium hydroxide in water (pH = 10, T = 20 °C) was carried out for 1 hour. By slow evaporation of the solvent, a powder/crystals having the unexpected stoichiometry $CsOH(CYH_3)_{1.3}$ was obtained. The crystal structure determination reveals that the asymmetric unit of the $Cs_3(CYH_3)_4(OH)_3$ (**2**) contains three independent Cs^+ cations that coordinate three OH^- ions each, and four cyanuric acid molecules in their keto tautomeric form (see Figures 6 – 8).

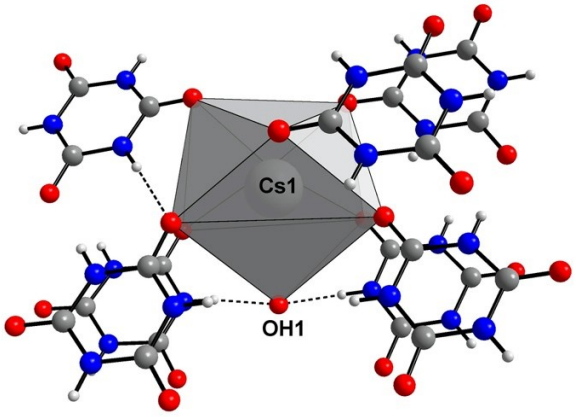

Fig. 6 The coordination environment about Cs1 in $Cs_3(CYH_3)_4(OH)_3$ (**2**)

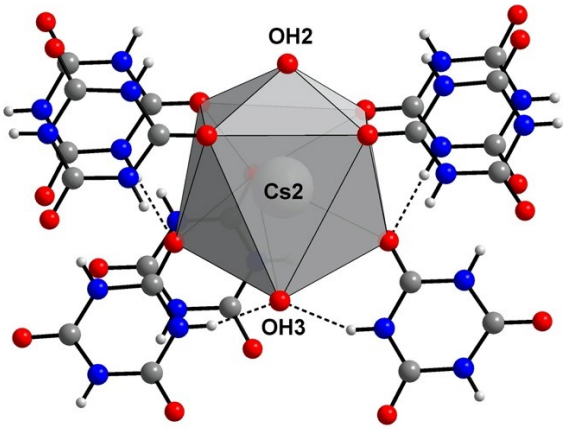

Fig. 7 The coordination environment about Cs2 in $Cs_3(CYH_3)_4(OH)_3$ (**2**)

View Article Online
DOI: 10.1039/D0NJ05601D

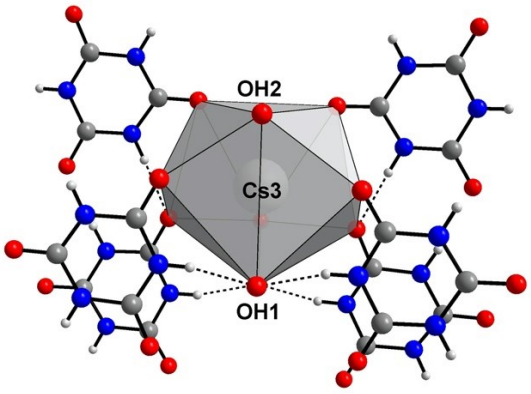

Fig. 8 The coordination environment about Cs3 in $Cs_3(CYH_3)_4(OH)_3$ (**2**)

Two of the Cs^+ cations (Cs1 and Cs2) display a nine-fold coordination with Cs-O distances in the range 3.007(9) – 3.823(13) Å and one (Cs3) is ten-fold coordinated with Cs-O distances in the range 3.161(14) – 3.653(17) Å. The Cs^+ cations with the OH^- anions are arranged to form layers intercalated by the coordinated cyanuric acid molecules. The main differences between the bond lengths of CYH_3 and those observed in **2** are found in the C-O bond length, which is appreciably lengthened in the latter compound, [CYH_3 average $d_{C\text{-}O}$ = 1.215; **2** average $d_{C\text{-}O}$ = 1.249 Å], as a consequence of the interaction of the oxygen atoms with the caesium ions. Conversely, the average C-N bond length in cyanuric acid and **2** are almost identical [CYH_3 ($d_{C\text{-}N}$ = 1.3660 Å); **2** ($d_{C\text{-}N}$ = 1.369 Å).[18] Two of the three N-H groups present in the CYH_3 molecule are involved in the formation of hydrogen bonds with C=O groups of adjacent molecules, while the third N-H group forms hydrogen bonds with the hydroxide anion, Table 2 and Figures 9 - 11.

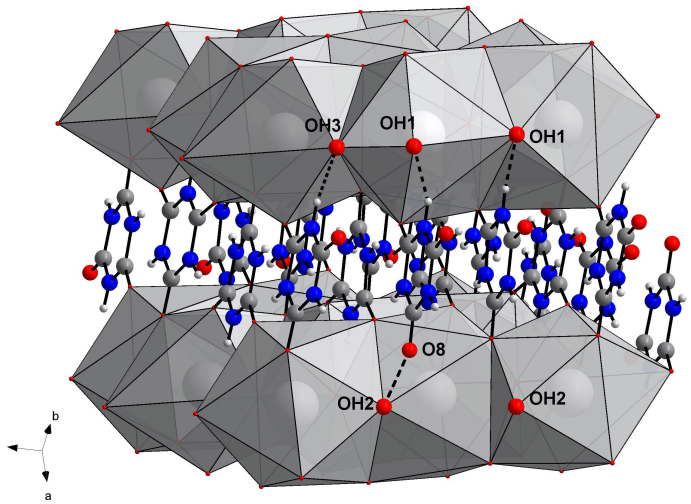

Fig. 9 Perspective view of two Cs layers held together by hydrogen bonding in $Cs_3(CYH_3)_4(OH)_3$ (**2**)

The cyanuric acid molecular flat ribbons (Figure 12) are formed through the extensive cyclic N-H···O hydrogen bonding interactions featuring a topological pattern of the type $R^2_2(8)$.[23] The observed N···O hydrogen bond distances (in the range 2.808 – 2.867 Å) are comparable to those of the reported cyanuric acid adducts,[22,24.] and CYH_3 (2.88 Å).[18, 25]

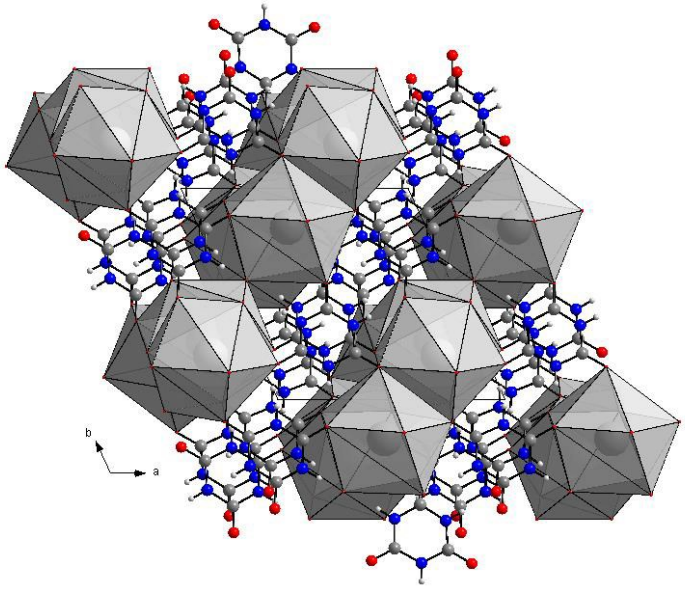

Fig. 10 Perspective view of $Cs_3(CYH_3)_4(OH)_3$ (**2**) seen along [001] with the Cs coordination polyhedra highlighted.

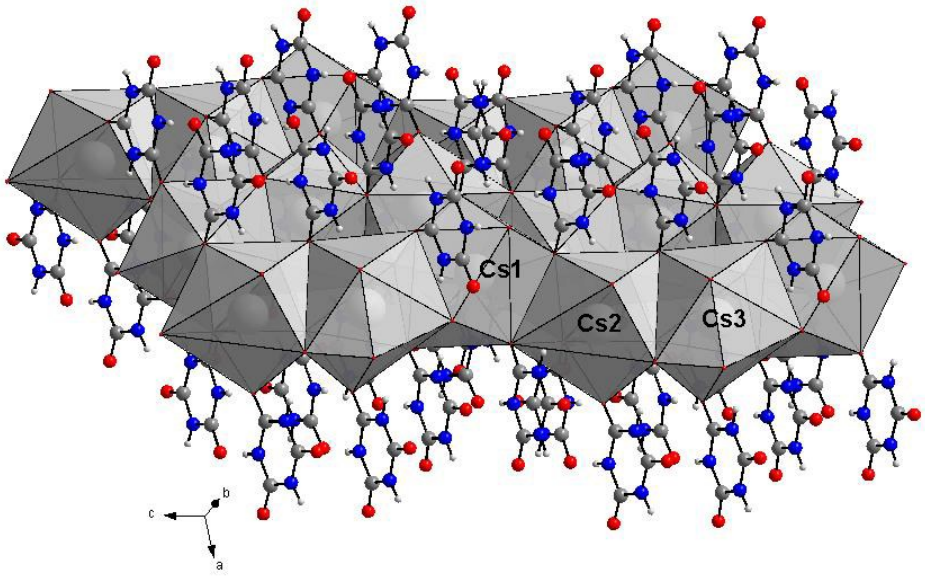

Fig. 11 A particular of $Cs_3(CYH_3)_4(OH)_3$ structure showing the arrangement of the cyanuric acid molecules about the Cs^+ ions.

View Article Online
DOI: 10.1039/D0NJ05601D

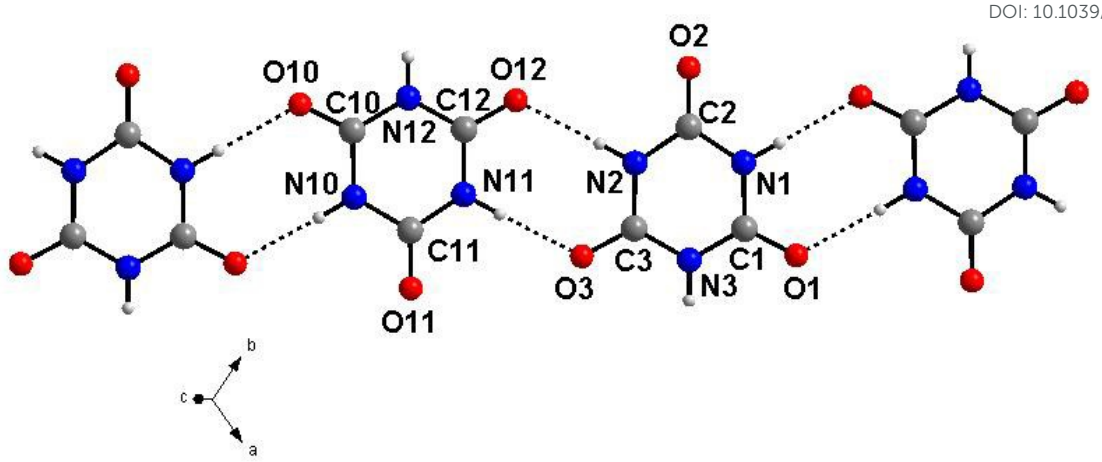

Fig. 12 Hydrogen-bonded CYH_3 molecules in (**2**) that form ribbons intercalated between layers of the Cs^+ ions. Interatomic distances (Å) are: C1-O1 1.248(13), C1-N1 1.391(15), C1-N3 1.340(14), C2-O2 1.251(15), C2-N1 1.384(14), C2-N2 1.368(14), C3-O3 1.250(14), C3-N2 1.386(15), C3-N3 1.357(13), C10-O10 1.237(13), C10-N10 1.411(14), C10-N12 1.365(14), C11-O11 1.236(15), C11-N10 1.375(13), C11-N11 1.361(14), C12-O12 1.251(13), C12-N11 1.384(14), C12-N12 1.355(13)

Table 2. Hydrogen bonds in $Cs_3(CYH_3)_4(OH)_3$ (**2**)

N4···O7a	2.765(14)	N4-H4···O7a	173(1)
N1···O10a	2.841(13)	N1-H1···O10a	179(1)
N7···O4a	2.838(14)	N7-H7···O4a	174(1)
N10···O1a	2.867(14)	N10-H10···O1a	175(1)
N5-O9b	2.906(15)	N5-H5···O9b	173(1)
N8···O6b	2.751(15)	N8-H8···O6b	177(1)
N2-O12b	2.846(15)	N2-H2···O12b	170(1)
N11-O3b	2.808(15)	N11-H11···O3b	177(1)
N3···OH3c	2.875(21)	N3-H3···OH3c	132(1)
N9-OH1d	2.671(22)	N9-H9···OH1d	157(1)
N12-OH3e	2.793(21)	N12-H12···OH3e	161(1)

Symmetry codes: a = -x, -y, -z; b = 1-x, 1-y, -z; c = -x, 1-y, -1-z; d = -x, 1-y, -z; e = x,y, 1+z; e = x-1, y, z; f = -x, 1-y, -z; g = x-1, y, z-1; h = -x, -y, -1-z; i = x,y,z-1; j = -1-x,-y,-1-z;

The ability of cyanuric acid molecules and cyanurates to self-assemble forming considerably stable flat ribbons is known in the literature.[26] It is reported that parallel molecular ribbons, spaced from each other between 6.71 to 17.75 Å, [22] can incorporate between them suitable guest molecules (DMSO, DMA, DMF, or metal complexes). As example, in the case of the compound cyanuric acid with $Cu(pic)_2(H_2O)$ [Hpic = picolinic acid] the copper complex molecules are inserted in such a way that each molecule forms two N···O hydrogen bonds with adjacent cyanuric acid molecules yielding a two dimensional layer with the distance between the cyanuric acid ribbons of 15.56 Å.[22] In

View Article Online
DOI: 10.1039/D0NJ05601D

compound **2**, the cyanuric acid units that make up the flat ribbons, stabilize the caesium cations *via* O···Cs^+ interactions and the hydroxide anions *via* N-H···OH hydrogen bonds. Compound **2** along with compound [CsLOH] L= 5,5-dimethyl-4-oxoimidazolidine-2-thione] [27] seems to be among the few compounds in which caesium hydroxide interacts with an organic weak-acid molecule to form an inorganic base-organic network. Both in compound [CsLOH] and (**2**), the organic moiety induces a major change in the network of $CsOH \cdot nH_2O$.[28] The observed effect is obtaining layers of CsOH interspersed with layers of hydrogen-bonded (iso)cyanuric acid molecules or 5,5-dimethyl-4-oxoimidazolidine-2-thione.

Conclusions

Both the oxalurate anion (OXL) and the cyanuric acid are small and simple organic molecules characterized by the presence of N-H, C=O, and COO^- functional groups that form strong hydrogen bonds in the solid state, with the separation N···O shorter than the sum of the relevant van der Waals radii. The salt Cs(OXL) was obtained from the reaction of parabanic acid with caesium hydroxide, whereas in the case of cyanuric acid, the separated solid $[Cs_3(CYH_3)_4(OH)_3]$ consists of co-crystals of CsOH and cyanuric acid in a ratio of 1:1.33. The reported X-ray crystal structures show that both the organic moieties form robust homomeric ribbons based on strong and articulated N-H···O hydrogen bonds. No water or other solvents are present in the two separated compounds to fulfill the required electronic charge to the Cs^+ ions. The high coordination number of caesium ions observed in the two structures involves average Cs-O bonding distances of about 3.26 Å while also ensures a more homogeneous distribution of the negative charge around the caesium atoms. The examination of the crystalline structures shows that the stabilization of the Cs^+ ion can occur regardless of whether the ribbon of organic units is negatively charged or neutral. The simultaneous presence of Cs^+ and OH^- ions in the cyanuric acid ribbon network provides information on how it is possible to stabilise an inorganic base with a simple organic molecule, although the latter contains dissociable protons. The molecular electrostatic potential maps have provided results consistent with the structural data, and have proved useful in visualizing the electronic charge distribution and related acceptor and donor capabilities of the molecule.

The interesting results obtained make it possible to hypothesize that systems of high complexity, such as humic acid and fulvic acid, featuring numerous oxygen atom-containing functional groups can easily stabilise caesium salts both in solution and in the solid state.

Conflicts of interest

There are no conflict to declare

Experimental

All reactants and solvents were used as purchased from Aldrich. Elemental analyses were obtained using a Perkin Elmer Series II - 2400. Infrared spectra were recorded with a Bruker Tensor 27 spectrometer equipped with a Platinum-ATR accessory and a DTGS detector. ^{1}H NMR spectra were obtained on a Varian Unity 400 at T = 21 °C, the ^{1}H chemical shifts were calibrated indirectly relative to $SiMe_4$.

Synthesis of Cs(oxalurate) (1). Parabanic acid (0.200 g, 1.75 mmol) was dissolved in water (20 mL). CsOH (50 wt % H_2O) was added drop by drop to the solution until a pH =10 was obtained; the mixture was stirred at 20°C for 1 hour. After that the clear solution was filtered (polyester syringe filter Chromafilm-Xtra PET 0.45 μm), and then slowly concentrated in desiccator (silica gel) under slight vacuum conditions to produce a white powder. Air stable suitable crystals were grown from slow evaporation of a hot solution of the powder dissolved in isopropyl alcohol. Yield 0.383 g, 83%; $C_3H_3CsN_2O_4$ M (263.98 g/mol): calcd C 13.65, H 1.15, N 10.61. Found: C 13.2, H 12, N 10.8. ^{1}H-NMR (400 MHz, DMSO-d_6) δ = 7.96 (2H), 7.85 (1H). IR (ν, cm^{-1}): 3401(s), 3277 (s), 3210 (s), 1745 (s), 1673 (m), 1603 (m), 1183 (m), 1114 (m), 785 (s), 605 (s), 590 (s).

Synthesis of $Cs_3(CYH_3)_4(OH)_3$ (2). Cyanuric acid (0.200 g, 1.55 mmol) was suspended in water (20 mL) and CsOH (50 wt % H_2O) drop by drop was added to the solution until a stable pH value of 10 was reached; the mixture was stirred at 20°C for 1 hour. After that the clear solution was filtered (polyester syringe filter Chromafilm-Xtra PET 0.45 μm), and then slowly concentrated in desiccator (silica gel) under slight vacuum conditions to produce a white powder. Air stable suitable crystals were grown from slow evaporation of a hot solution of the powder dissolved in isopropyl alcohol. Yield 0.291 g, 78 %; $C_{12}H_{15}Cs_3N_{12}O_{15}$ M (966.09 g/mol): calcd C 14.92, H 1.56, N 17.40. Found: C 15.1, H 1.6, N 18.0. ^{1}H-NMR (400 MHz, DMSO-d_6) δ = 9.5. IR (ν, cm^{-1}): 2836(w), 1727(s), 1700(s), 1551(s), 1477(m), 1379(vs), 1345(s), 883(w), 838(m), 780(s), 759(w), 700(w), 689(w), 550(s), 421(w).

X-ray structure determination

A summary of the crystal data and refinement details for compounds (**1**) and (**2**) is given in ESI-Table S1. Intensity data were collected at room temperature on a Bruker Apex II CCD diffractometer using graphite-monochromatized Mo-Kα radiation (λ = 0.71073 Å). Datasets were corrected for Lorentz-polarization effects and for absorption (SADABS)[29]. Both structures were solved by direct methods

(SIR-92)[30] and completed by iterative cycles of full-matrix least squares refinement on Fo^2 and ΔF synthesis using the SHELXL-2017/1 program[31] (WinGX suite)[32]. Hydrogen atoms, located on the ΔF maps, were also included in the refinement. Crystals of compound (**2**) were invariably needle-like aggregates with no chance to obtain single crystal fragments after cleavage. The high R value obtained at the end of the refinement, the systematic presence of a large number of reflections having Fo>Fc and the high value of the second weight parameter were among the symptoms that the crystal used for the diffraction experiment was partly twinned. The PLATON/TwinRotMat [33] software revealed that the crystal is a non-merohedral twin. Twin refinement was therefore applied with the twin matrix |-1 0 0 0 -1 0 0.882 0.689 1| which resulted in a slight lowering of the R factor from 0.108 to 0.086. An attempt to improve the quality of the collected data with a NEEDLE absorption correction didn't gave better results and ghost peaks close to the heavier atoms and at chemically impossible positions still remained. Nevertheless, the formulation and the structural features of compound (**2**) are unambiguously established. Selected interatomic distances and angles for (**1**) and (**2**) are reported in the supplementary information Tables S2 and S3, respectively. Crystallographic data for both compounds have been deposited with the Cambridge Crystallographic Data Centre as supplementary publication no. CCDC 2039762-2039763. These data can be obtained free of charge via www.ccdc.cam.ac.uk/conts/retrieving.html (or from CCDC, 12 Union Road, Cambridge CB2 1EZ, UK; fax: +44 1223 336033; e-mail: deposit@ccdc.cam.ac.uk.

Computational studies

Geometry optimization of OXL and di-OXL ions were performed on an Intel-i7 based system using Spartan'14, Wavefunction inc., using B3LYP as the density functional theory functional and 6-31G** for the basis set. IR frequency calculations were carried out to verify the nature of the minima of each optimization by assessing the absence of calculated negative frequencies. Heat of formation, electron density surface, atomic, electrostatic[34], natural[35] , Mulliken charges[36], and HOMO and LUMO orbitals were also calculated. SM8 solvation model was used. Geometries were optimized in gas phase and in solution (water).[37]

Notes and references

1 (*a*) P. J. White, M. R. Broadley, *New Phytol.* **2000**, 147, 241-256; (*b*) P. Li, Y. Gong, M. Komatsuzaki, *Science of the Total Environment*, **2019**, 697, Article 134060; (*c*) R. Pöllänen, I. Valkama, H. Toivonen, *Atmospheric Environment*, **1997**, 31, 3575-3590; (*d*) Stohl, P. Seibert, G. Wotawa, D. Arnold, J. F. Burkhart, S. Eckhardt, C. Tapia, A. Vargas, T. J. Yasunari, *Atmos. Chem. Phys.*, **2012**, 12, 2313, 2343; (*e*) U.S. Department of Health and Human Services, Agency for Toxic Substances and Disease registry: Toxicological Profile for Cesium; April 2004.

2 (*a*) F. J. Stevenson, *Humus Chemistry*, *Genesis, Composition, Reactivity*, 2nd ed.; John Wiley & Sons: New York, 1984; (*b*) R. Sutton, G. Sposito, *Environmental Science & Technology*, **2005**, 39, 9009-9015.

3 (*a*) H. R. Schulten, M. Schnitzer, *Naturwissenschaften*, **1993**, 80, 29-30; (*b*) O. Celebi, A. Kilikli, H. N. Erten, *J. Haz. Mat*., **2009**, 168, 695-703.

4 (*a*) S. Trevisan, O. Francioso, S. Quaggiotti, S. Nardi, *Plant Signaling & Behaviour*, **2010**, 5:6, 635-643; (*b*) T. J. Yasunari, A. Stohl, R. S. Hayano, J. Burkhart, S. Eckhardt, T. Yasunari, *PNAS*, **2011**, 108, 19530-19534.

5 (*a*) C. Mayeux, J. Tammiku-Taul, L. Massi, J. F. Gal, P. Burk, *ChemPlusChem*, **2013**, 78, 1195-1204; (*b*) C. R. Hampton, H. C. Bowen, M. R. Broadley, J. P. Hammond, A. Mead, K. A. Payne, J. Pritchard, P. J. White, *J. Plant Physiol*., **2004**, 136, 3824-3837; (*c*) N. C. Brady, R. R. Weil, The Nature and Properties of Soils. Prentice Hall, Inc., Upper Sadle River, New Jersey, USA, 1999.

6 (*a*) P. Boguta, Z. Sokolowska, *Molecules*, **2020**, 25(6), article number 1297; (*b*) M. A. Ashraf, S. Akib, M. J. Maah, I. Yusoff, K. Balkhair, *Critical Reviews in Environmental Science and Technology*, **2014**, 44, 1740-1793.

7 (*a*) H. -S. Shieh, D. Voet, *Acta Crystallogr., Sect.B:Struct.Crystallogr.Cryst.Chem.*, **1975***,* 31, 2192-2201; (*b*) A. C. Wang, B. M. Craven, *Acta Crystallogr., Sect.B:Struct.Crystallogr.Cryst.Chem.,***1979**, 35, 510-513; (c) L. R. Falvello, R. Garde, M. Tomas, *Inorg.Chem.*, **2002**, 41, 4599-4604; (d) Lian-Feng Zhang, *Acta Crystallogr.,Sect.E:Struct.Rep.Online ,***2007**, 65**,** m308; (e) T. Kavitha, G. Pasupathi, M. K. Marchewka, G. Anbalagan, N. Kanagathara, *J.Mol.Struct.*, **2017**, 1143, 378-383 .

8 L. R. Falvello, I. Pascual, M. Tomás, E. P. Urriolabeitia, *J. Am. Chem. Soc*., **1997**, 119, 11894-11902.

9 K. M. Fromm, *Coord. Chem Rev.,* **2008**, 252, 856-885.

10 Inorganic Chemistry Structure Database, Fachinformationszentrum, Karlsruhe, Germany.

11 A. Leclaire *J. Solid State Chem.,* **2008**, 181, 2338-2345.

12 E. Scrocco, J. Tomasi, *Topics Curr Chem*., **1973**, 42, 95-170; E. Scrocco, J. Tomasi, *Adv Quantum Chem*., **1978**, 11, 115-193.

13 J. S. Murray, P. Politzer, *WIREs Comput. Mol. Sci.*, **2011**, 1, 153-163.

14 P. Politzer, M. C. Concha, J. S. Murray, *Int. J. Quantum Chem.,* **2000**, 80, 184-192.

15 IUPAC name: 1,3,5-Triazine-2,4,6(1*H*,3*H*,5*H*)-trione

16 G. S. Nichol, W. Clegg, M. J. Gutmann, D. M. Tooke, *Acta Cryst*. **2006**, B62, 798-807.

17 I. M. Klotz, T. Askounis, *J. Am. Chem. Soc.,* **1947**, 69, 801-803.

18 E. H. Wiebenga, *J. Am. Chem. Soc.,* **1952**, 74, 6156-6157.

19 L. M. Perdigão, N. R. Champness, P. H. Beton, *Chem. Commun*., **2006**, 538-540.

20 G. B. Seifer, *Russian Journal of Coordination Chemistry*, **2002**, 28, 301-324.

21 S. Aoki, M. Shiro, T. Koike, E. Kimura, *J. Am. Chem. Soc*., **2000**, 122, 576-584.

22 A.-Q Wu, G.-H Guo, F.-K Zheng, X. Liu, G.-C Guo, J.-S. Huang, *Inorganic Chemistry Communications*, **2005**, 8, 182-185.

23 M. C. Etter, *Acc. Chem. Res*., **1990**, 23, 120-126

24 V. R. Pedireddi, D. Belhekar, *Tetrahedron*, **2002**, 58, 2937-2941

25 P. Coppens, A. Vos, *Acta Crystallogr.,* **1971**, B27, 146-158.

26 (*a*) L. Zhou-Bin, C. Chang-Zhang, G. Dong-Shou, H. Xiao Ying, L. Ding, *Jiegou Huaxue(Chin.) Chin. J Struct. Chem*., **1995**, 14, 61; (b) X. Lu, J. Gao, L. Gai, D. Cui, Q. Wang, *Heterocycles*, **2008**, 75, 2443-2458; (*c*) S. J. Makowski, E. Calta, M. Lacher, W. Schnick, *Z. Anorg. Allg, Chem.,* **2012**, 638, 88-93.

27 M. Arca, F. Demartin, F. A. Devillanova, A. Garau, F. Isaia, V. Lippolis, G. Verani, *Inorg. Chem.*, **1998**, 37, 4164-4165.

28 H. Jacobs, B. Harbrecht, P. Müller, W. Bronger,., *Z. anorg. Allg. Chem.,* **1982**, 491, 154-162.

29 SADABS Area-Detector Absorption Correction Program, Bruker AXS Inc. Madison, WI, USA, 2000.

30 A. Altomare, M. C. Burla, M. Camalli, G. L. Cascarano, C. Giacovazzo, A. Guagliardi, A. G. G. Moliterni, G. Polidori, R. Spagna R, *J. Appl. Cryst.,* **1999**, 32, 115-119.

31 G.M. Sheldrick, SHELXL- Programs for Crystal Structure Analysis (Release 2017/1); University of Göttingen, Germany,

32 L. J. Farrugia, *J. Appl. Crystallogr.,* **1999**, 32, 837-838.

33 A.L.Spek, (1980-2020) Utrecht University, Padualaan 8, 3584 CH Utrecht, The Netherlands.

34 L. E. Chirlian, M. M. Francl, *J. Comput. Chem*., **1987**, 8, 894-905; (b) C. M. Breneman, K. B. Wiberg, *J. Compt. Chem*., **1990**, 11, 361-373.

35 A. E. Reed, R. B. Weinstock, F. Weinhold, *J. Chem. Phys*., **1985**, 83, 735-746.

36 R. S. Mulliken, J. *Chem. Phys.,* **1955**, 23, 1833-1840; (b) R. S. Mulliken, J. *Chem. Phys.,* **1955**, 23, 2338-2342.

37 A. V. Marenich, R. M. Olson, C. P. Kelly, C. J. Cramer, D. G. Truhlar, *J. Chem. Theory, Comput.,* **2007**, 3, 2011-2033.